Warm Dark Matter and its astrophysical signatures

Peter L. Biermann[1,2,3,4]

July 22, 2015; Meeting at Paris

[1] MPI for Radioastronomy, Bonn, Germany;
[2] Dept. of Phys., Karlsruhe Inst. for Tech. KIT;
[3] Dept. of Ph. & A., Univ. of Alabama, Tuscaloosa, AL, USA;
[4] Dept. of Phys. & Astron., Univ. Bonn;
with help by with Biman B. Nath (RRI Bangalore),

Laurenţiu I. Caramete (ISS Bucharest, MPIfR Bonn), Ben C. Harms (UA Tuscaloosa), Eberhard Haug (Univ. Tübingen), Paul Mason (Univ. NM), Athina Meli (Univ. Gent), Felix Mirabel (Buenos Aires, Paris), Todor Stanev (Bartol, Delaware), & Julia Becker Tjus (Univ. Bochum)

Hector de Vega - in memoriam

Challenges

- 1 Evidence for dark matter
- 2 Anti-matter: Energetic positrons
- 3 Anti-matter: Anti-protons
- 4 DM-decay? X-ray data
- 5 The neutrino horizon
- 6 Very early star formation: HD absorption
- 7 Early Super-Massive Black Holes

Evidence for dark matter

- Clusters of galaxies (Zwicky 1933)
- Galaxy rotation curves (Rubin)
- Stability of galactic disks (Ostriker, Peebles)
- Matching MWBG fluctuations (Planck 2013):

  $\Omega_\Lambda = 0.692 \pm 0.010$

  $\Omega_{dm} = 0.2582 \pm 0.0047$ DARK MATTER

  $\Omega_b = 0.0482 \pm 0.00076$

  $\Omega_k = 1 - \Omega_\Lambda - \Omega_{dm} - \Omega_b = -0.0005 \pm 0.0066$

  $->$ "flat" geometry, like a perfect tabletop
- Ell. gal., e.g. NGC5846 (PLB et al. 1983)
- Dwarf elliptical galaxies (Hogan & Dalcanton and very many later papers)

Evidence for dark matter in galaxies

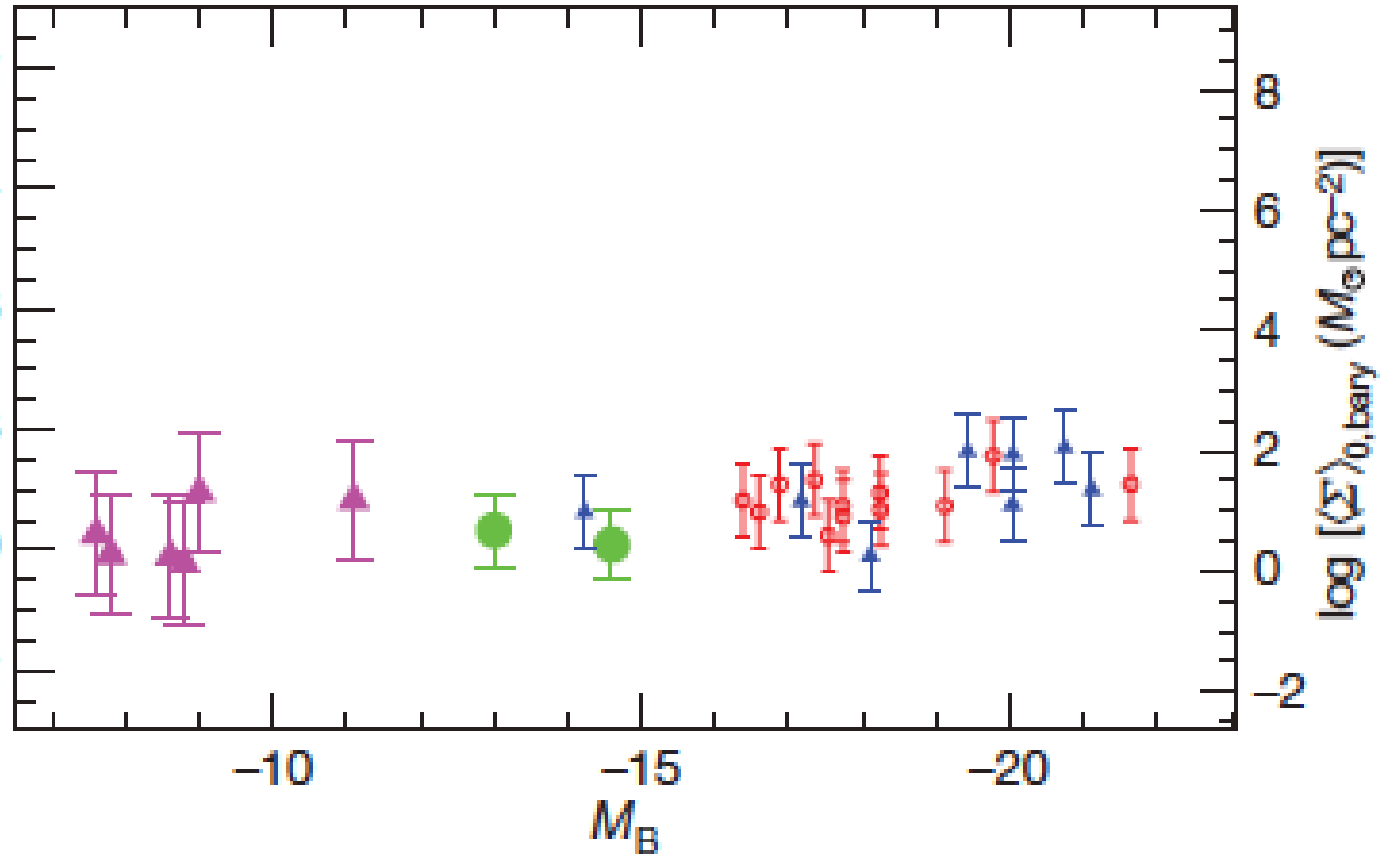

Figure 1 The central surface density in galaxies. Source: Gentile et al. 2009 Nature

Latest AMS results

- Protons
- Electrons
- Positrons: secondary
- Anti-protons: secondary
- Helium
- Carbon
- B/C ratio: B secondary
- Lithium: mostly secondary

Evidence for DM particle decay in these data?

AMS Positrons

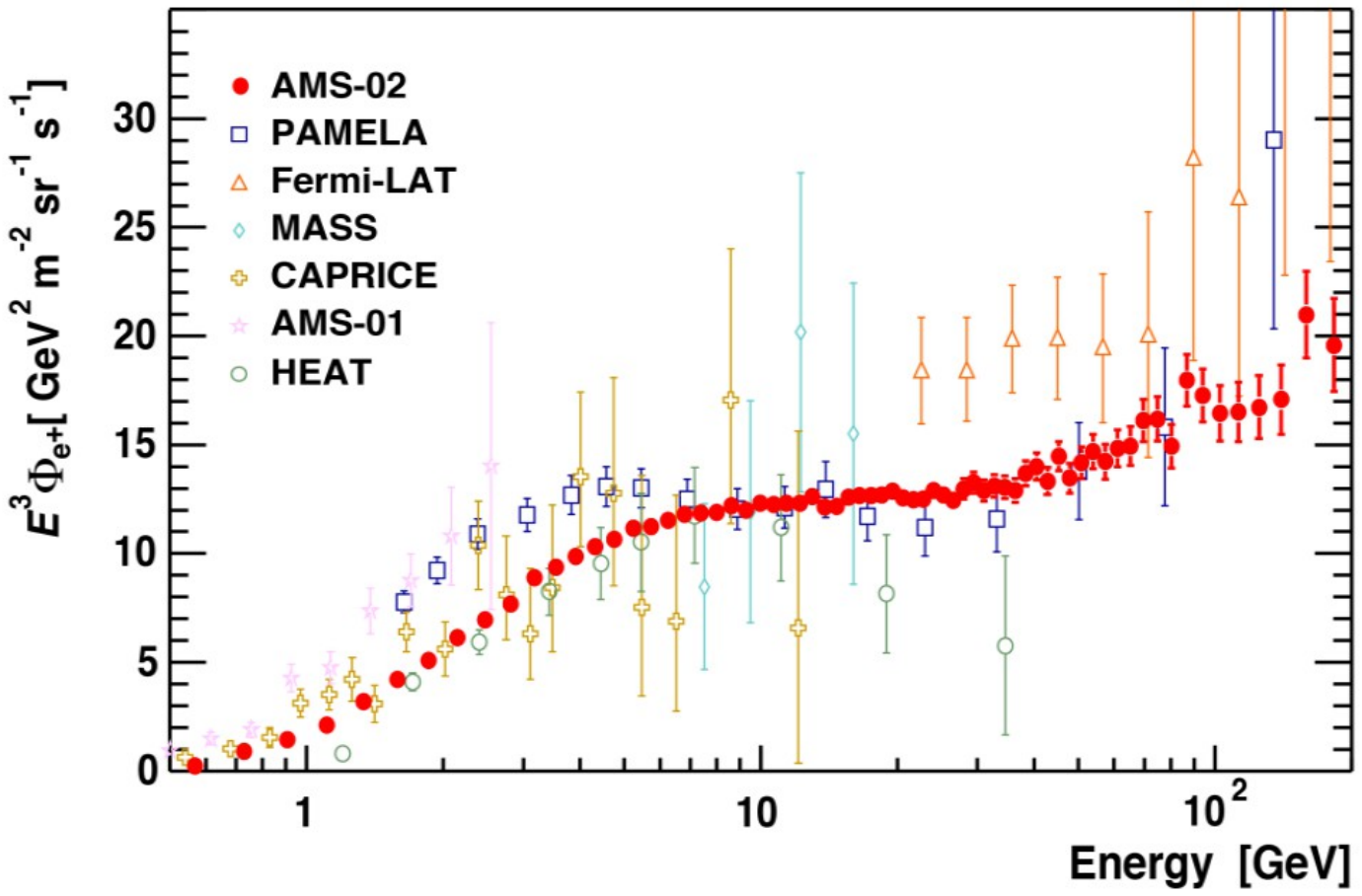

Figure 2 AMS positrons. Source: AMS-CERN Ting lecture Apr 2015

Positrons: triplet pair production I

- Total **cross-section for triplet pair production**

  $\boldsymbol{\sigma_{3,tot} = \alpha r_0^2 \left(\frac{28}{9} \ln\{2k\} - \frac{218}{27} + \frac{1}{k}\text{terms}\right)}$

  with $\alpha r_0^2 = 10^{-27.3}\,\text{cm}^2$

  $\boldsymbol{k = (h\nu \cdot E_e)/(m_e c^2)^2}$, with $\boldsymbol{k = 2}$ threshold.

- Using 3.0 eV and 30 TeV gives then as total cross-section (using just the first term) $\mathbf{10^{-26.05}\,cm^2}$

- **Distort CR-e spectrum** $\boldsymbol{\sigma_{3,tot}\tau_{CR}cn_{ph} = 1/3.}$

- In OB-superbubble photon density condition

$$\frac{\tau_{CR}}{10^6\,\text{yrs}} \; \frac{n_{ph}}{10^{1.7}\,\text{cm}^{-3}} > 1$$

just **somewhat higher than in the GC region.**

Interstellar radiation field

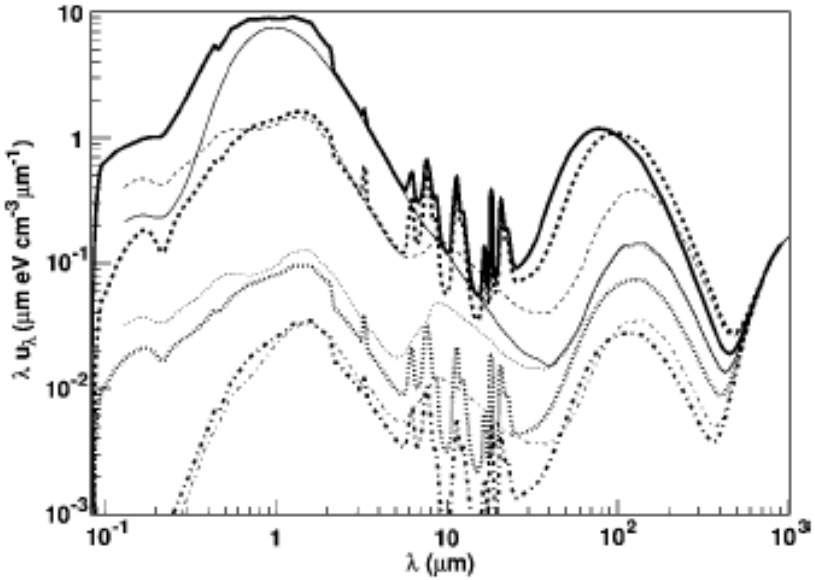

FIG. 1.—Interstellar radiation field energy density. *Top*: Local interstellar radiation field. *Thick solid line*, total radiation field including CMB; *thick dashed line*, contribution by stars; *thick dotted line*, scattered light; *thick dot-dashed line*, infrared; *thin solid line*, local ISRF from Strong et al. (2000). Data: *Squares*, *Apollo* (Henry et al. 1980); *triangles*, DIRBE (Arendt et al. 1998); *circles*, FIRAS (Finkbeiner et al. 1999). *Bottom*: Interstellar total radiation field radial variation. *Solid lines*, $(R, z) = (0 \text{ kpc}, 0 \text{ kpc})$; *dashed lines*, $(R, z) = (4 \text{ kpc}, 0 \text{ kpc})$; *dotted lines*, $(R, z) = (12 \text{ kpc}, 0 \text{ kpc})$; *dash-dotted lines*, $(R, z) = (16 \text{ kpc}, 0 \text{ kpc})$. Thick lines are for our ISRF; thin lines are for the ISRF of Strong et al. (2000).

Figure 3 Interstellar radiation field in Galactic Center region; we assume here that in a OB-superbubble the radiation is similar, but yet more intense, and perhaps slightly bluer. Source: Moskalenko & Strong 2006 ApJL 640, L155, 2006

Positrons: triplet pair production II

- The Red Super-Giant (RSG) stars have a slow wind, with instabilities leading to shock-waves giving $\boldsymbol{k^{-2}}$ turbulent wave-field spectrum, so already at low energy **secondary spectrum unchanged** from primary spectrum (PLB et al. 2009).
- **Secondary CR-e^+ from p-p collisions original spectrum**, so same as primaries. Most interaction in polar cap (PLB et al. 2009). Triplet pair production additional.
- Graph: Positrons from the triplet-pair production using $\boldsymbol{(h\nu) = 3.0}$ **eV,** $\boldsymbol{E_{e,max} = 30}$ **TeV, and electron-spectrum with slope** $\boldsymbol{\delta = 2}$. Work with **Eberhard Haug 2014** (priv.comm.)

Triplet-pair production of positrons

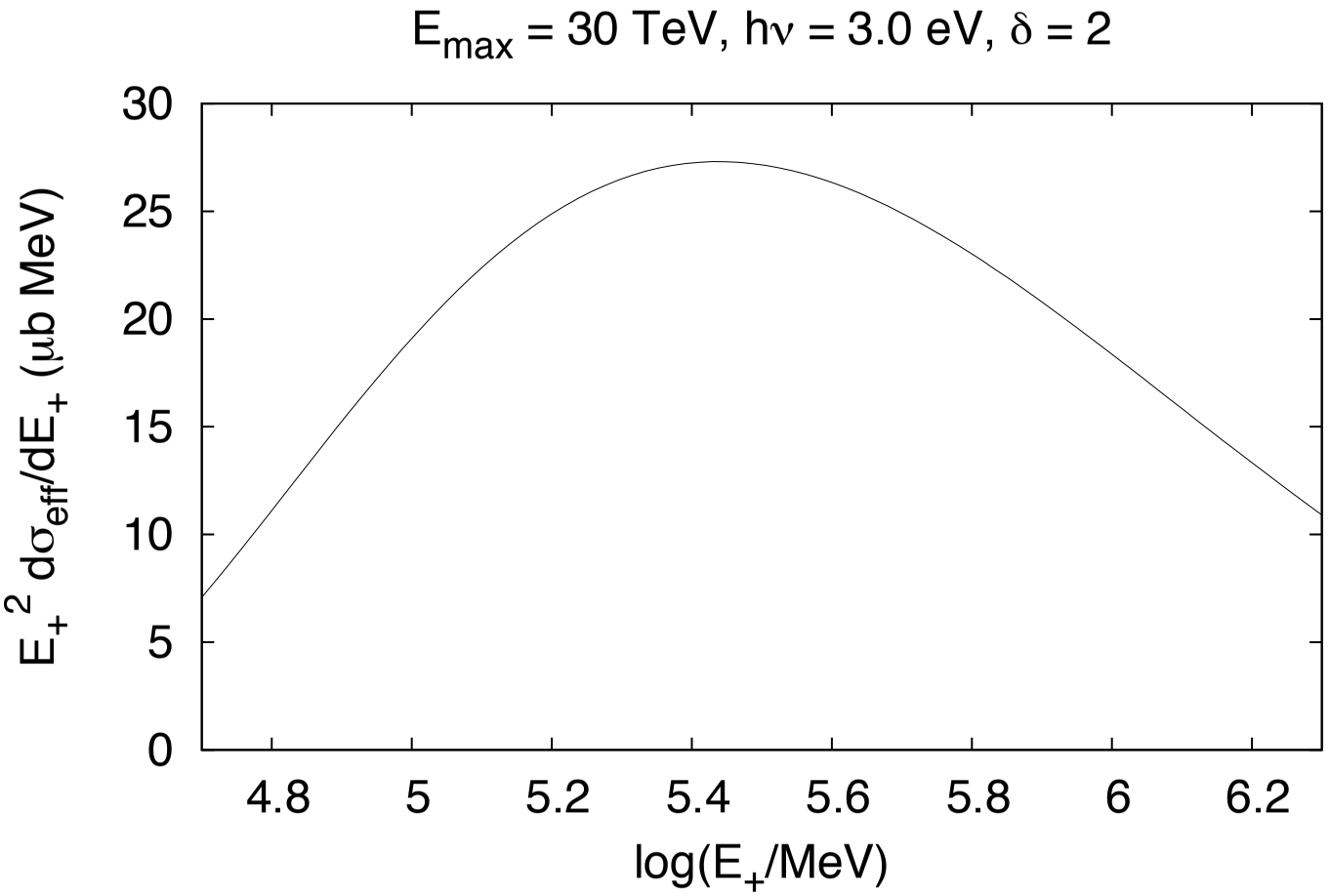

Figure 4 Positrons from the triplet-pair production using $(h\nu) = 3.0$ eV, $E_{e,max} = 30$ TeV, and electron-spectrum with slope $\delta = 2$. Source: Eberhard Haug 2014

AMS Anti-proton fraction

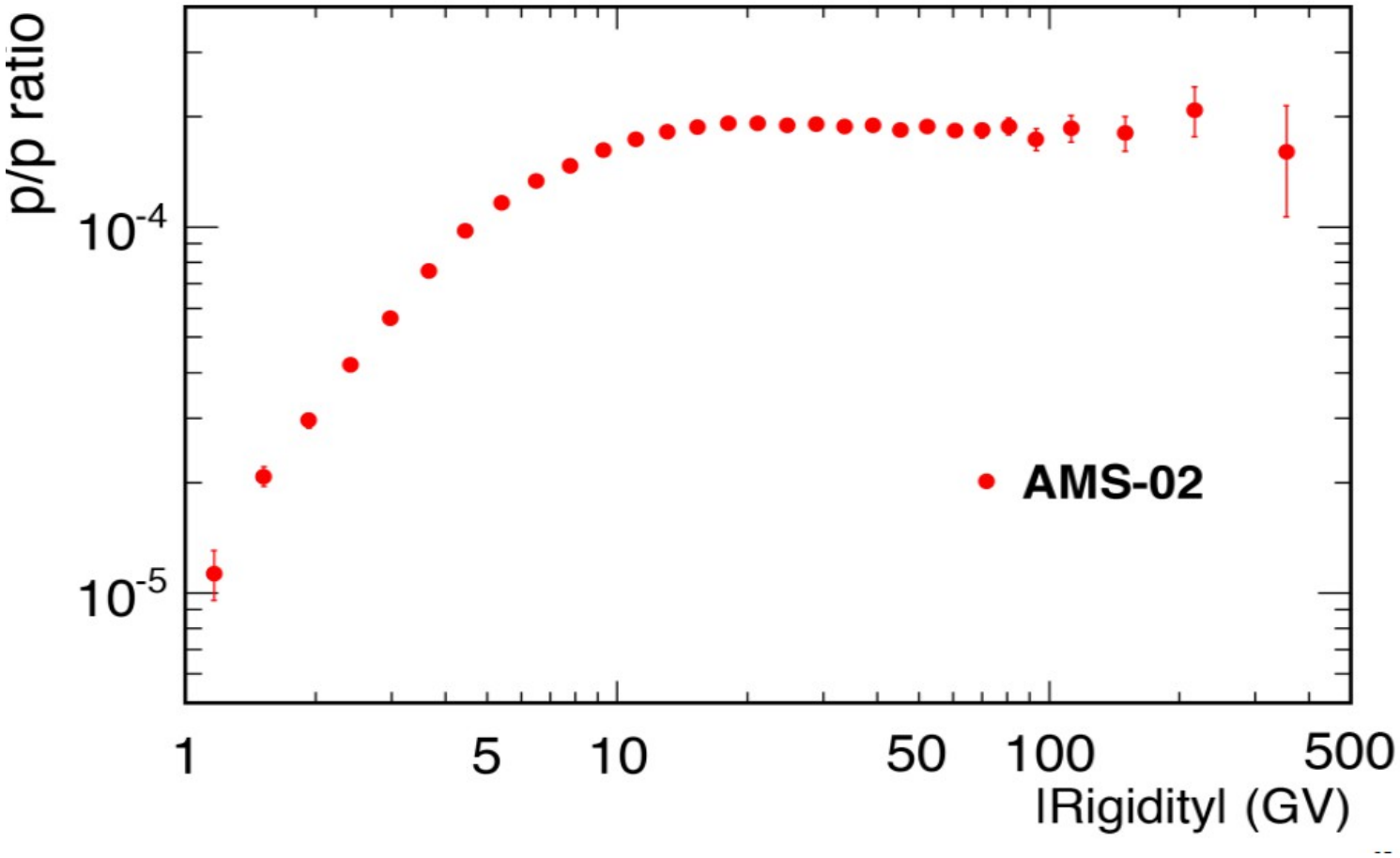

Figure 5 AMS antiproton fraction. Source: AMS-CERN Ting lecture Apr 2015

AMS Anti-proton fraction - numbers I

- Anti-protons: **First match ISM-CR-protons and RSG-wind-CR-protons, cross-over around TeV**
- Protons AMS fit: $\boldsymbol{E^{-2.82\pm0.01}}$
- Test CR-wind component with AMS-Helium
- Predicts for Red Super-Giant (RSG) stars already at low energy secondaries same spectrum as primaries (PLB et al. 2009).
- This implies that anti-proton to proton ratio runs as

$$\frac{F_{\bar{p}}(E)}{F_p(E)} = \frac{a_{ISM,sec}\,E^{-3.15} + a_{RSG,sec}\,E^{-2.67}}{a_{ISM,prim}\,E^{-2.82} + a_{RSG,prim}\,E^{-2.67}}$$

AMS Anti-proton fraction - numbers II

- Just crudely fitting first the AMS proton data and then the anti-proton data allows for the three parameters:
- $\boldsymbol{a_{ISM,sec}/a_{RSG,prim} = 5. \cdot 10^{-5}}$,
- $\boldsymbol{a_{ISM,sec}/a_{RSG,prim} = 4. \cdot 10^{-4}}$, **and**
- $\boldsymbol{a_{ISM,prim}/a_{RSG,prim} = 1.3}$
- using as reference energy 100 GeV. With these specific parameter examples the anti-proton fraction varies a few percent from 10 GeV to 300 GeV. **Upper limit for $\boldsymbol{a_{ISM,sec}/a_{RSG,prim}$ - small**.

AMS Anti-proton fraction - prediction

- **Maxwell's laws** require that over some small fraction over a spherically symmetric surface in a wind the magnetic field is radial. Polar cap in real space or in phase space: E^{-2} **at source**
- Transition energy E_{trans} for WR stars observed at a few TeV; if same for RSG stars $E_{trans} = 5$ TeV
- The **interactions in polar cap have more time by** A, and so **transition of secondaries** of polar cap component is shifted down by A^{-3}.
- Anti-proton to proton ratio changes to $E^{+1/3}$ **behavior from about** $165\,(A/3)^{-3}\,(E_{trans}/\{5\mathrm{TeV}\})$ **GeV to** E_{trans}**, and then approaches a constant again**.

Latest AMS results: Evidence for DM decay ?

- Positrons: secondary
- Anti-protons: secondary

No evidence for DM particle decay in these data !

X-ray evidence ? $2 \times 3.55\,\mathrm{keV}$ seen

- Assume **sterile neutrino** of a few keV, based on dwarf elliptical galaxies and cores of larger galaxies:
- **Decay** into left-handed neutrino and **X-ray photon**
- **Phase-space distribution**: Fermi-Dirac with tail
- **Integrate** for density law, and gravitational field
- **Predict** radial run of X-ray emissivity
- **Iterate** to obtain match to observational data: detection or limit
- **Problem:** Phase-space distribution may **not** be **isotropic**
- **Problem: Outer regions of clusters** of galaxies **not** in **hydrostatic equilibrium**

X-ray evidence ? Why Perseus strongest ?

- Sterile neutrino mass and mixing angle measurements obtained from our samples.
- Compared with the limits placed by the single well exposed Bullet cluster (Boyarsky et al. 2008) and and Andromeda galaxy (Horiuchi et al. 2014)
- The line in Perseus is much brighter than expected

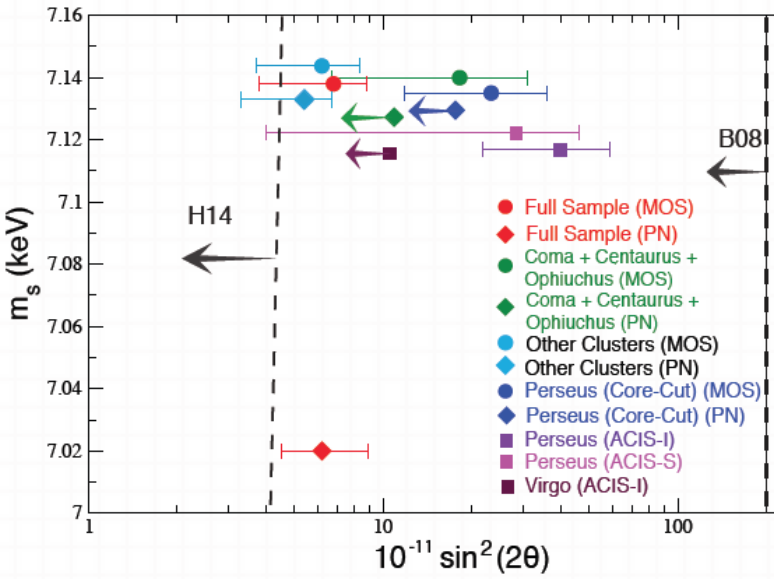

Sterile neutrino mass and mixing angle measurements and upper limits obtained from the different samples.

Figure 6 Limits on X-ray detection. **Perseus is strongest, WHY ? Perhaps, because the cluster is merging and has three central galaxies with a SMBH, NGC1270 and NGC1277, apart from the dominant galaxy NGC1275** (Bosch et al., Fabian et al.). Source Esra Bulbul lecture 2014.

Why Perseus strongest ? WDM simulations !

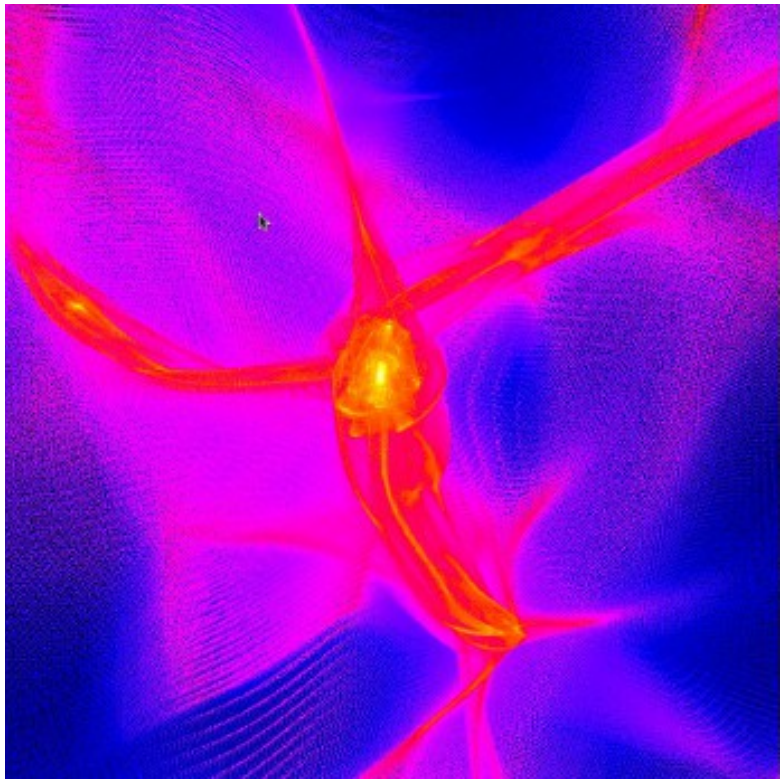

Figure 7 WDM simulations, shown here in 2D projection; this shows that line of sight integrations would show **large variations from various directions**, easily consistent with the observed data. Source **Sinziana Paduroiu** lecture Meudon 2015.

Star formation in the early Universe

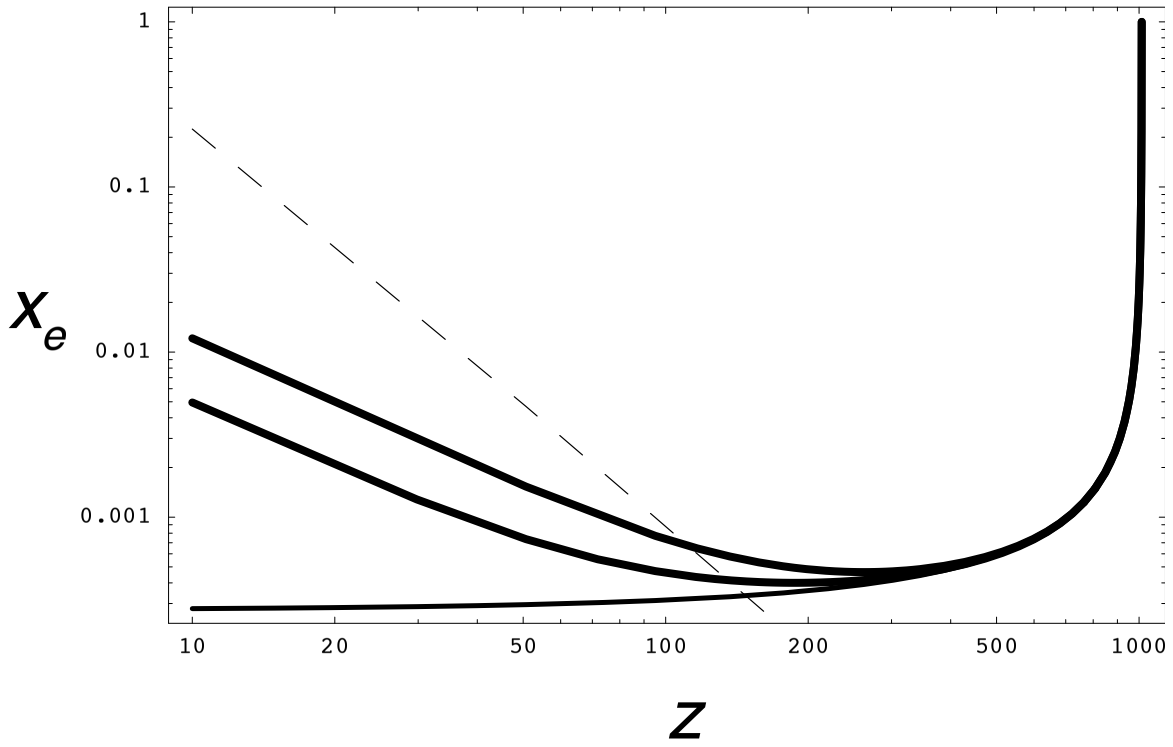

Figure 8 Degree of ionization in the early universe for different assumed masses of the **DM sterile neutrino, here 4 and 7 keV**; **extra ionization leads to stronger formation of molecular Hydrogen.. Molecular Hydrogen allows strong cooling, and this in turn allows early star formation**. Source PLB & Kusenko 2006 PRL.

Star formation near redshift 100

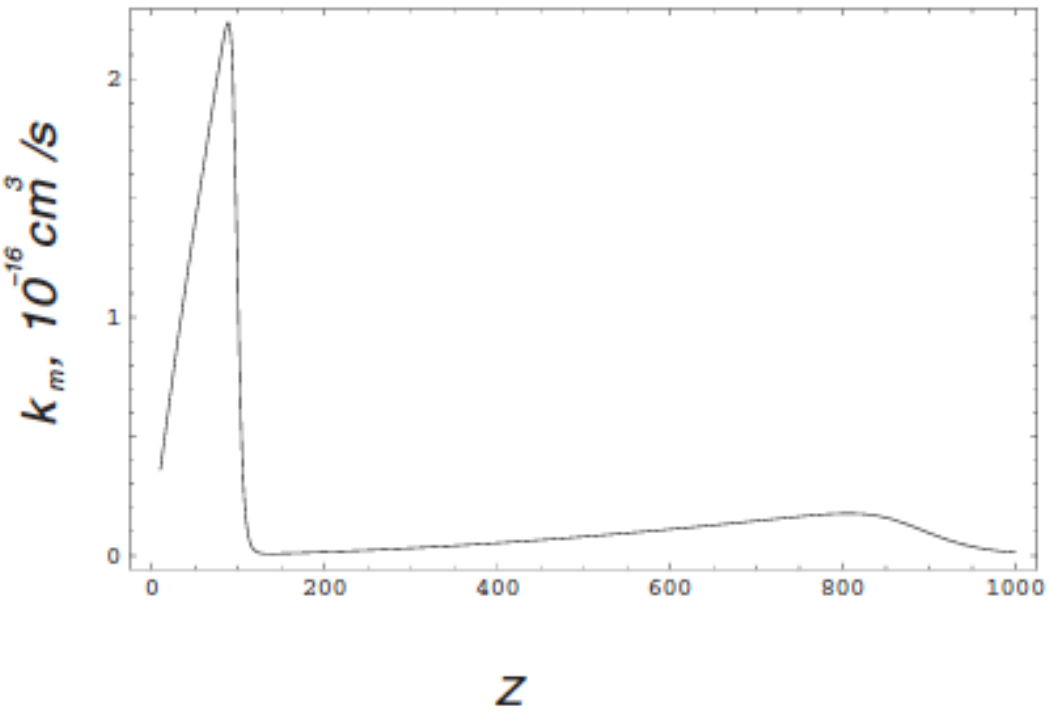

Figure 9 **Molecular Hydrogen cooling function** coefficient for different assumed masses of the DM sterile neutrino; this allows extreme cooling and **star formation**. Source PLB & Kusenko 2006 PRL.

Star formation observed/derived

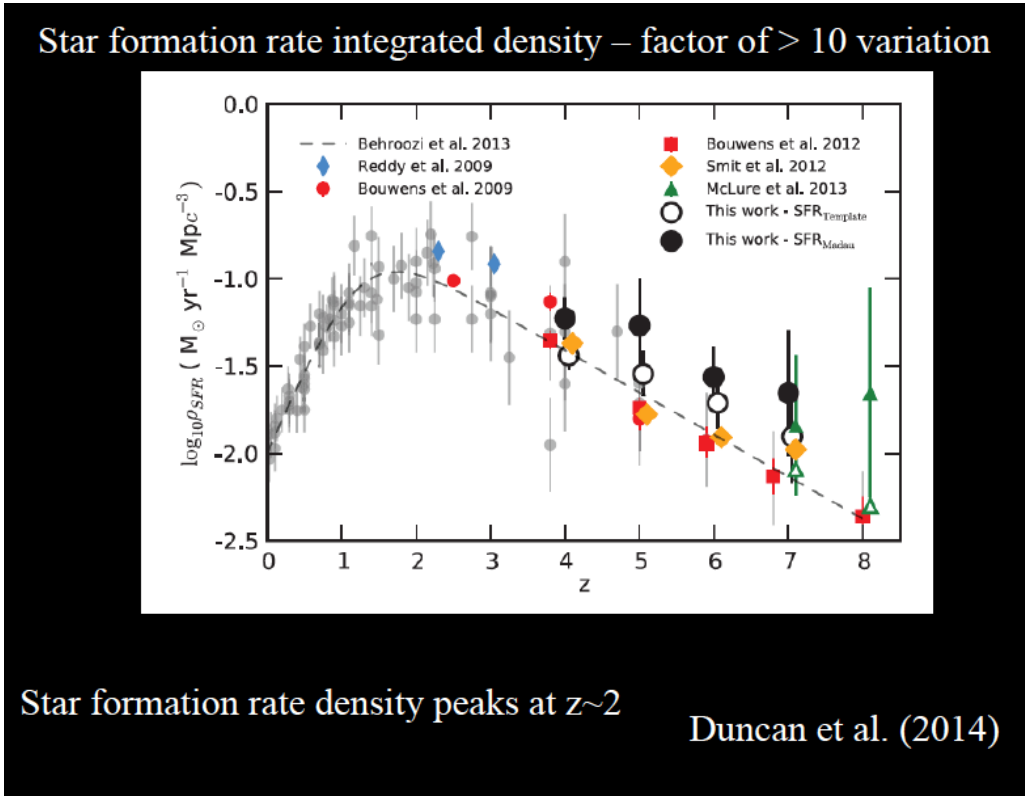

Figure 10 Star formation at high redshift, to z about 8. Source Chris Conselice Lecture Paris 2014.

Star formation observed/limits

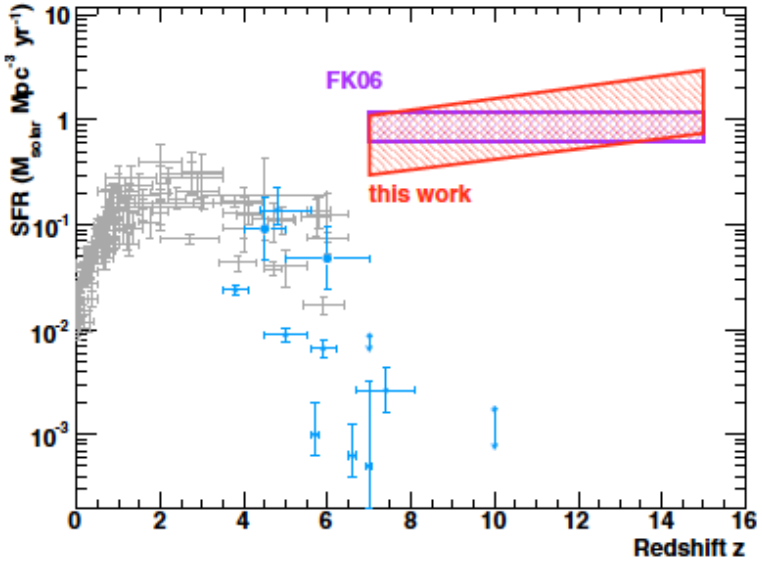

Fig. 11. Limits on the co-moving SFR of PopIII stars derived in this paper in comparison to other limits and measurements of the star formation rate. The purple striped region indicates the range given in FK06 (see text for details). Blue open markers are from the data collection from Yüksel et al. (2008), while blue filled markers at $z = 4.5$ and $z = 6$ are the data points derived in the same paper from GRB measurements. As a reference for the low redshift SFR the data collection from Hopkins & Beacom (2006) is given (grey markers).

Figure 11 Star formation limits at high redshift, to z about 15. Source Raue et al. AA 498, 25, 2009.

Star formation from BH density

- SMBH density $\mathbf{10^{-1.7\pm0.4}\,Mpc^{-3}} > 3{\cdot}10^6\,M_\odot$ now
- If growth by early merging, originally $\mathbf{10^{-1.2\pm0.4}\,Mpc^{-3}}$
- Baryons today: $10^{+9.7}\,M_\odot\,Mpc^{-3}$
- Efficiency to make stars $10^{-4}\,\epsilon_{-4}$, need volume $10^{+0.8}\,\epsilon_{-4}^{-1}\,Mpc^{+3}$ to make SMBH of $\mathbf{3\cdot10^6\,M_\odot}$ – **our original**
- If stars turn 1/3 via agglomeration into SM star, then SMBH, expected density $\mathbf{10^{-1.3}\,\epsilon_{-4}^{-1}\,Mpc^{-3}}$
- Redshift 100 z_2, so timescale of $10^{7.2}z_2^{-3/2}$ yrs, star formation rate $\mathbf{10^{-1.5}\,\epsilon_{-4}^{-1}\,z_2^{+3/2}\,M_\odot\,yr^{-1}\,Mpc^{-3}}$
- **If SMBH growth from DM** (Munyaneza & PLB 2005/6), then only **weak constraints** here

Early stars via HD molecules: 1 to 10 μ

TABLE I. Measured wavelengths of lines, where $P(J'')$, $Q(J'')$, and $R(J'')$ have the usual meaning of a rotational transition, in the $B^1\Sigma_u^+ - X^1\Sigma_g^+$ Lyman bands (indicated as Lv) and $C^1\Pi_u - X^1\Sigma_g^+$ Werner bands (indicated as Wv) for HD with the Amsterdam narrow band extreme ultraviolet laser facility and the K_i coefficients as calculated. The typical uncertainty in the measured wavelengths is $\Delta\lambda = 0.000\,005$ nm, while that in the sensitivity coefficients is $\Delta K_i = 0.000\,15$.

Line	λ_0 (nm)	K_i	Line	λ_0 (nm)	K_i
L0P1	110.729 245	−0.007 89	L6R3	103.536 700	0.020 64
L0P2	110.911 618[a]	−0.009 69	L6R4	103.790 376	0.018 31
L0P3	111.166 568[a]	−0.012 11	L7P1	102.262 976	0.027 22
L0R0	110.584 055	−0.006 54	L7P2	102.425 462	0.025 51
L0R1	110.621 689	−0.006 96	L7P3	102.656 725	0.023 18
L0R2	110.732 767	−0.008 11	L7R0	102.146 045	0.028 31
L1P1	109.340 155	−0.001 73	L7R1	102.191 899	0.027 78
L1P2	109.519 532	−0.003 47	L7R2	102.307 083	0.026 44

Figure 12 The lines of HD in nm, so typically 1000 Angstrom; redshifts 10 to 100 correspond then to **wavelengths of 1 to 10 μ**. Source Ivanov et al. 2008 PRL 100, 093007.

HNR Thomson depth and polarization

The observed Thomson depth is about $10^{-1.05}$; integral

$$\int x_e(z')\,\sigma_T\,n_0(1+z')^3\,\frac{c}{(1+z')H(z')}dz'$$

- Integral $x_e(z') = 1$ to redshift 6 not enough.
- Many HNRs, ϵ UV-Eddington-fraction:

$$\tau_{Th,sum} = 10^{-1.7}\left(\frac{1+z}{51}\right)^4\left(\frac{M_{SMS}}{10^{6.5}M_\odot}\right)\epsilon_{-0.5}$$

- HNRs highly magnetized, lateral scale about 25 arc-sec: non-thermal emission **highly polarized**

Degenerate islands ?

- Momentum phase space degenerate up to $m_{DM}\sigma$
- Condition of full degeneracy

$$\frac{4\pi}{3}R^3\frac{4\pi}{3}(m_{DM}\sigma)^3\frac{2}{\hbar^3} = \frac{M_{island}}{m_{DM}}$$

- In numbers

$$R^3_{kpc}\left(\frac{\sigma}{c}\right)^3 = 10^{-22}\,M_{\odot^8}$$

- **Test** with Oppenheimer-Volkov (OV) limit and $\sim$ 5 Schwarzschild radii at $\sigma/c = 1$
- **Island formation** at very high redshift? **Prelude to clumping, star and SMBH formation ?**

Where are the sources? IceCube 2014

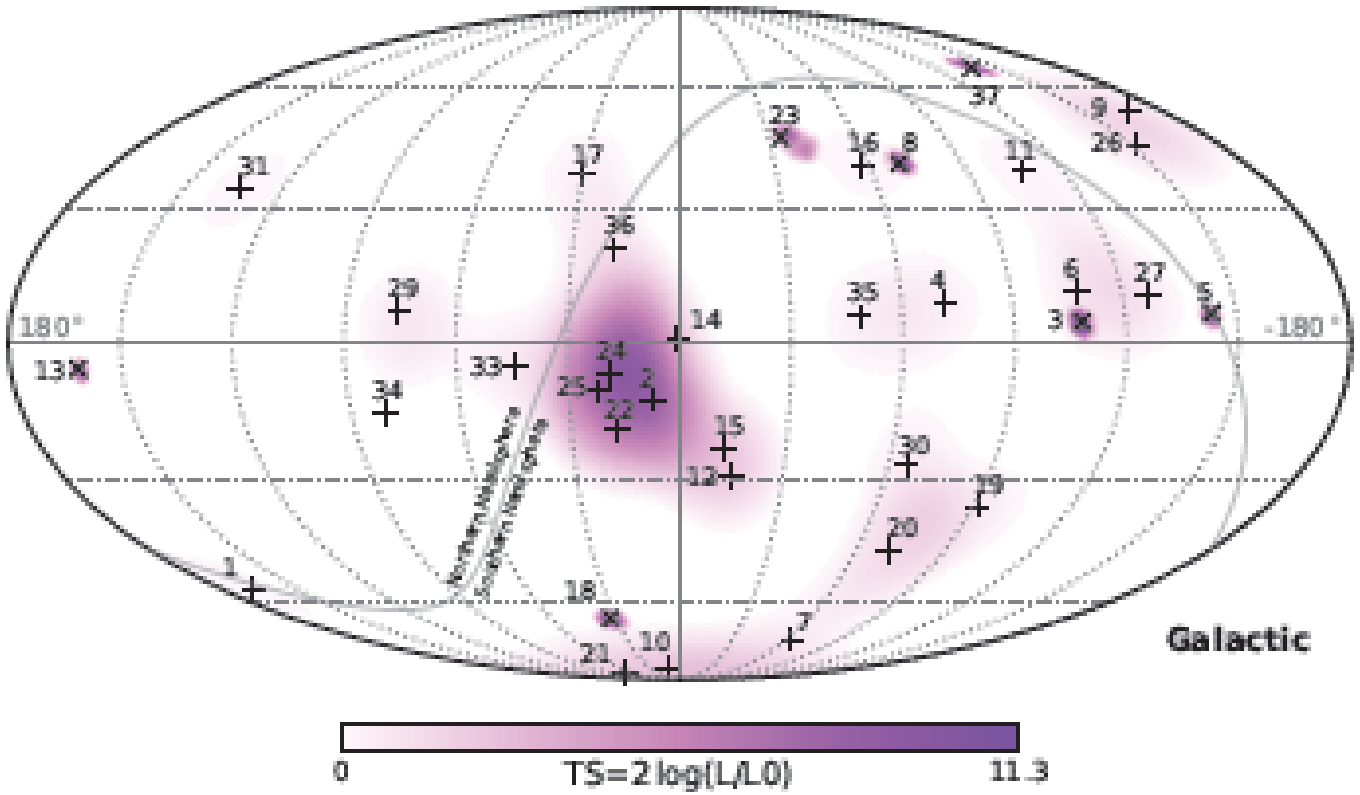

Figure 13 The HE neutrino events 2014. GC at center. Source PRL .

Neutrino $z_{sources} \sim 2$, or $>> 2$

$\lesssim$ **50 Mpc**: Some ? Or low redshift, max $\sim$ **2** :

$$F_\nu \sim \int N_z \, z^2 \, \frac{L}{z^2} \, dz \sim \Delta z,$$

Normal sources $N_z \sim (1+z)^3$, $z_{sources} \sim 2$
Some classes N_z inversely with heavy elements Z:

$$F_\nu \sim \int N_z \frac{L}{(1+z)^{7/2}} \, dz \sim \int \frac{N_z \, L \, dt}{(1+z)},$$

For Δt fixed lifetime $\Delta z \sim (1+z)^{5/2} \Delta t$ stronger contribution at very high redshift, for $N_z \sim (1+z)^{1+\epsilon}$ for $\epsilon > 0$; $\int L \, dt$ fixed, $->$ $z_{sources} >> 2$:

Are neutrino sources visible at $z < 100$?

- **z up to 100** possible for first star formation (PLB & Kusenko 2006 PRL), **key enhanced H_2 cooling**
- **High energy neutrinos interact !**
- **$\Omega_b = 0.0482 \pm 0.00076$** (Planck 2013 XVI)
- Baryonic mass density $\rho_{bar} \sim (1+z)^3$
- Radiation energy density $\rho_{rad} \sim (1+z)^4$
- Work with **Todor Stanev 2015** (priv.comm.)
- For PeV neutrinos: **Maximum redshift about 18**
- So, if observed spectrum cuts off at PeV, then sources probably **at higher redshift**; if observed spectrum continues, redshift **below this limit !**

Odd coincidence

- What energy ejected **forming black hole**? Limit (1/2) rest mass energy for spin zero BH. Budget

$$\frac{1}{2}\, N_{BH,0}\, M_{BH}\, c^2 (1+z_\star)^3 \sim 10^{-8}\,\mathrm{erg/cc}$$

- as **DE**, for $N_{BH,0} = 1\, Mpc^{-3}$, $M_{BH} = 3 \cdot 10^6\, M_\odot$, $z_\star = 50$: **Gravitational waves?**
- Large **uncertainties** in 1/2, $N_{BH,0}$, M_{BH}, and $z_\star$.
- **Einstein and conserv. eqs. in 5D, analytical solution**. Work with **Ben Harms 2015** (priv.comm.).
- Energy transfer from **strong brane** (Planck density) to **weak brane** (us) mimics e.o.s. $P = -\rho\, c^2$!

  IF so, prediction: detectable GW bg !

QUESTIONS: Early universe visible ?

- keV sterile neutrinos allow very early star and BH formation, from $z \lesssim 100$
- Neutrinos ? $z \simeq 2$ or $z >> 2$, and $z < 18$
- Radio background ?
- Low frequency GW background from BHs ?
- Massive shells $->$ Massive disk galaxies ?
- Test I: Identify the HE ν-sources !
- Test II: Get z from HD absorption !
- Test III: Detect first SMBH activity !

Thank you!